Systemic antithrombotic effects of ADAMTS13

Anil K. Chauhan,[1,2] David G. Motto,[3] Colin B. Lamb,[1] Wolfgang Bergmeier,[1,2] Michael Dockal,[5] Barbara Plaimauer,[5] Friedrich Scheiflinger,[5] David Ginsburg,[4] and Denisa D. Wagner[1,2]

[1]CBR Institute for Biomedical Research and [2]Department of Pathology, Harvard Medical School, Boston, MA 02115
[3]Department of Pediatrics, University of Michigan, and [4]Department of Internal Medicine, University of Michigan and Howard Hughes Medical Institute, Ann Arbor, MI 48109
[5]Baxter Bioscience, Vienna, A-1220 Austria

The metalloprotease ADAMTS13 (a disintegrin-like and metalloprotease with thrombospondin type I repeats 13) cleaves highly adhesive large von Willebrand factor (VWF) multimers after their release from the endothelium. ADAMTS13 deficiency is linked to a life-threatening disorder, thrombotic thrombocytopenic purpura (TTP), characterized by platelet-rich thrombi in the microvasculature. Here, we show spontaneous thrombus formation in activated microvenules of *Adamts13*$^{-/-}$ mice by intravital microscopy. Strikingly, we found that ADAMTS13 down-regulates both platelet adhesion to exposed subendothelium and thrombus formation in injured arterioles. An inhibitory antibody to ADAMTS13 infused in wild-type mice prolonged adhesion of platelets to endothelium and induced thrombi formation with embolization in the activated microvenules. Absence of ADAMTS13 did not promote thrombi formation in αIIbβ3 integrin-inhibited blood. Recombinant ADAMTS13 reduced platelet adhesion and aggregation in histamine-activated venules and promoted thrombus dissolution in injured arterioles. Our findings reveal that ADAMTS13 has a powerful natural antithrombotic activity and recombinant ADAMTS13 could be used as an antithrombotic agent.

CORRESPONDENCE
Denisa D. Wagner:
wagner@cbr.med.harvard.edu

Abbreviations used: ADAMTS, a disintegrin-like and metalloprotease with thrombospondin type I repeats; r-hu, recombinant human; TTP, thrombotic thrombocytopenic purpura; UL-VWF, ultra-large VWF; VWF, von Willebrand factor.

Thrombotic thrombocytopenic purpura (TTP) is a disorder characterized by thrombotic microangiopathy, thrombocytopenia, and microvascular thrombosis that can cause various degrees of tissue ischemia and infarction. Clinically, TTP patients are diagnosed by signs and symptoms such as thrombocytopenia, microangiopathic hemolytic anemia, neurological abnormalities, renal failure, and fever (1, 2). In 1982, Moake et al. found ultra-large von Willebrand factor (UL-VWF) multimers in the plasma of patients with chronic relapsing TTP (3). Most patients suffering from TTP are deficient in a plasma metalloprotease that cleaves UL-VWF (4–9). The protease belongs to the ADAMTS (a disintegrin-like and metalloprotease with thrombospondin type I repeats) family and is designated as ADAMTS13, a 190-kD glycosylated protein produced predominantly by the liver (10–12), specifically by hepatic stellate cells (13, 14). Mutations in the ADAMTS13 gene have been shown to cause familial TTP (10). Acquired TTP, often caused by autoantibodies inhibiting ADAMTS13 activity, is a more common disorder that occurs in adults and older children and can recur at regular intervals in 11–36% of patients (4, 6). Nonneutralizing autoantibodies have been associated with acute acquired TTP (15). In most patients with familial or acquired TTP, plasma ADAMTS13 activity is absent or <5% of normal. Without treatment, the mortality rate exceeds 90%, but plasma exchange therapy has reduced mortality to ~20% (2).

VWF synthesized in megakaryocytes and endothelial cells is stored in platelet α-granules and Weibel-Palade bodies, respectively, as UL-VWF (16). Once secreted from endothelial cells, these UL-VWF multimers are cleaved by ADAMTS13 in the circulation into a series of smaller multimers at specific cleavage sites within the VWF molecule (17–19). The protease cleaves at the Tyr842–Met843 bond in the central A2 domain of the mature VWF subunit (20) and requires zinc and calcium for activity. VWF exists in "ball of yarn" and filamentous

The online version of this article contains supplemental material.

The Journal of Experimental Medicine

Table I. Hemodynamic parameters were established before application of A23187 (Fig. 1) on venules and $FeCl_3$ on arterioles (Fig. 5)

Genotype	Vessel type	Diameter (μm)	Centerline velocity (mm/s)	Shear rate (s^{-1})
Adamts13$^{+/+}$ ($n = 5$)	Venule	31.51 ± 1.79	1.43 ± 0.07	213 ± 14.10
Adamts13$^{-/-}$ ($n = 5$)	Venule	26.36 ± 1.95	1.28 ± 0.13	244 ± 28.29
Adamts13$^{+/+}$ ($n = 12$)	Arteriole	103.91 ± 9.29	33.33 ± 1.72	1,688.16 ± 143.32
Adamts13$^{-/-}$ ($n = 12$)	Arteriole	93.26 ± 10.48	28.05 ± 2.10	1,646.83 ± 157.16

forms as seen by electron microscopy (21). Furthermore, atomic force microscopy confirms that VWF exists in a globular conformation under static conditions and may unfold to a filamentous state after exposure to shear stress (22). This could occur also in vivo when one end of the VWF filament is anchored to a surface. UL-VWF multimers have high biological activity. They bind better to the extracellular matrix than regular multimers (23) and form higher strength bonds with platelet GPIb-IX than plasma VWF (24). It was demonstrated in vitro that platelets align as beads on the released UL-VWF string on the endothelial surface. These strings are then cleaved by ADAMTS13 and released from the stimulated endothelial cells (25). We have demonstrated in vivo that it is only in *Adamts13*$^{-/-}$ mice that strings of platelets remain intact after endothelial activation in veins (26). These strings attach at one end to endothelium and "wave" the other end in the blood stream.

Thrombi of TTP patients consist of a little fibrin but mainly of VWF and platelets, suggesting VWF-mediated platelet aggregation as a cause of thrombosis (27). We hypothesized that endothelial activation resulting in elevation of hyperactive UL-VWF multimers in plasma could be associated with an increased risk of thrombosis in ADAMTS13-deficient animals. We investigated thrombosis in venules and arterioles of *Adamts13*$^{-/-}$ mice by intravital microscopy. Our findings strongly suggest that ADAMTS13 has natural antithrombotic activity and that recombinant human (r-hu) ADAMTS13 could be used to treat TTP and possibly other thrombotic conditions.

RESULTS

Endothelial activation results in thrombi formation in microvenules of *Adamts13*$^{-/-}$ mice

We have previously observed that platelet sticking/translocation in venules of 200–250 μm in diameter activated with calcium ionophore A23187 (a secretagogue of Weibel-Palade bodies) at low shear rate (~100 s^{-1}) was prolonged in *Adamts13*$^{-/-}$ mice compared with *Adamts13*$^{+/+}$ mice (26). We investigated whether activation of microvenule endothelium by A23187 (which does not denude the endothelium; reference 28) results in platelet aggregation and subsequent thrombus formation. The shear rate (200–250 s^{-1}) and diameter of all the microvenules (25–30 μm) studied were similar for *Adamts13*$^{-/-}$ and *Adamts13*$^{+/+}$ mice (Table I). In the microvenules of *Adamts13*$^{-/-}$ mice, platelet aggregation resulting in thrombus formation was observed from 45 s to 2 min after topical superfusion of A23187 (Fig. 1). The thrombi were often unstable and flushed away, leading to frequent embolization and causing transient downstream occlusion usually only lasting 3–4 s. Thus, stimulation of Weibel-Palade body secretion can lead to spontaneous thrombus formation in *Adamts13*$^{-/-}$ mice in the absence of vascular injury. In *Adamts13*$^{+/+}$ mice treated identically, platelet strings and very small platelet aggregates could be seen attached to the

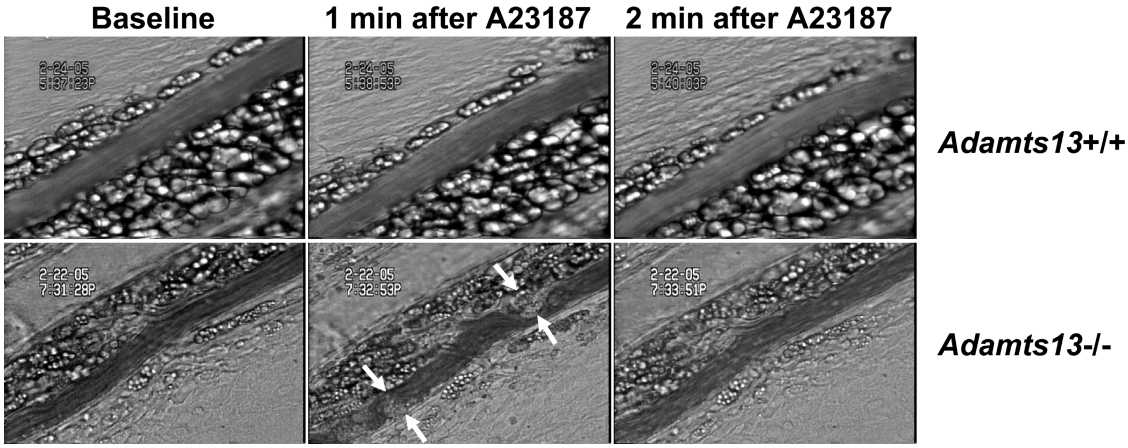

Figure 1. Thrombus formation in stimulated microvenules of *Adamts13*$^{-/-}$ mice. Venules measuring ~25–30-μm in diameter were visualized in the mesentery of live mice. 1 min after topical superfusion of calcium ionophore A23187, thrombus formation was observed in *Adamts13*$^{-/-}$ mice ($n = 5$). No microthrombi formed in *Adamts13*$^{+/+}$ mice treated identically ($n = 5$). Arrows indicate the microthrombi. See Video 1 (available at http://www.jem.org/cgi/content/full/jem.20051732/DC1) for thrombi in the microvenules of *Adamts13*$^{-/-}$ mice.

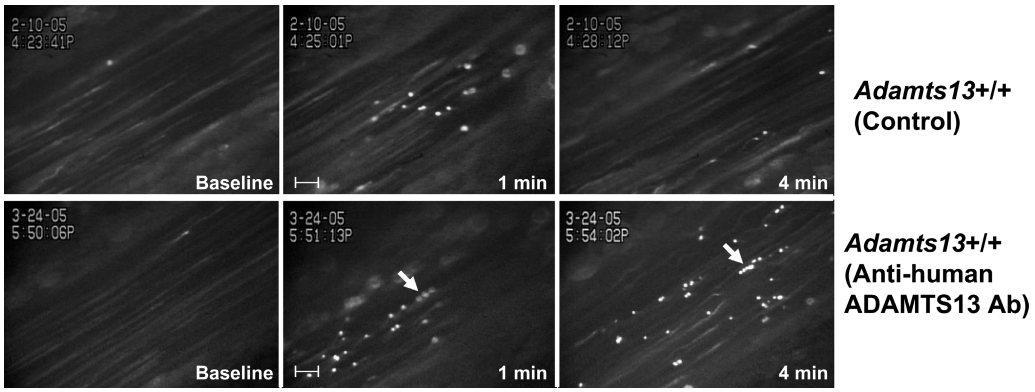

Figure 2. Antibody to ADAMTS13 increases platelet adhesion and string formation on activated vessel wall. Fluorescently labeled platelets representing ~2.5% of total platelets were observed in mesenteric venules (diameter: 200–250 μm) of live mice before (baseline) and after A23187 superfusion. Platelets began to adhere to the endothelium 30–45 s after superfusion. In *Adamts13*$^{+/+}$ mice (infused with anti–human ADAMTS13 Ab, $n = 4$), more platelets adhered to the vessel wall 4 min after stimulation compared with *Adamts13*$^{+/+}$ control ($n = 4$). Arrows indicate the ≥20-μm strings of platelets attached at one end to the endothelium and waving the other end in the blood stream. Inset time points in the lower right corner refer to the time after superfusion of A23187. The bar shown in the middle panel is ~50 μm.

endothelium for 1–2 s, but thrombi did not form. These observations demonstrate that ADAMTS13 is active at low shear and, thus, inhibits platelet aggregation and prevents thrombus formation in the microvenules. In addition, arterioles (high shear) running parallel to the venules in either *Adamts13*$^{-/-}$ or *Adamts13*$^{+/+}$ mice did not show any platelet strings, platelet aggregation, or thrombus formation.

An antibody to ADAMTS13 prolongs adhesion of platelets to secreted VWF on the vessel wall of *Adamts13*$^{+/+}$ mice

Previous studies have shown that most patients suffering from the acquired form of TTP have autoimmune inhibitors to ADAMTS13 in plasma (4, 6). We infused a polyclonal anti–human ADAMTS13 antibody in *Adamts13*$^{+/+}$ mice 2 h before surgical preparation for intravital microscopy. The antibody did not activate the endothelium as normal baseline platelet adhesion was found in *Adamts13*$^{+/+}$ mice after its infusion (Fig. 2). After topical superfusion of A23187, many platelets stuck/translocated on the endothelium, reaching a peak of platelet adhesion from 45 s to 1 min that progressively decreased with time. However, more platelet sticking was observed 4 min after the A23187 application in the antibody-infused *Adamts13*$^{+/+}$ as compared with control *Adamts13*$^{+/+}$ mice (control IgG [$n = 2$] or PBS [$n = 5$]) (Fig. 2). The phenomenon observed was similar to that observed in *Adamts13*$^{-/-}$ mice (26). Strings of platelets were seen varying from 20 to 40 μm and attached at one end to the endothelium and waving in the blood stream. These strings

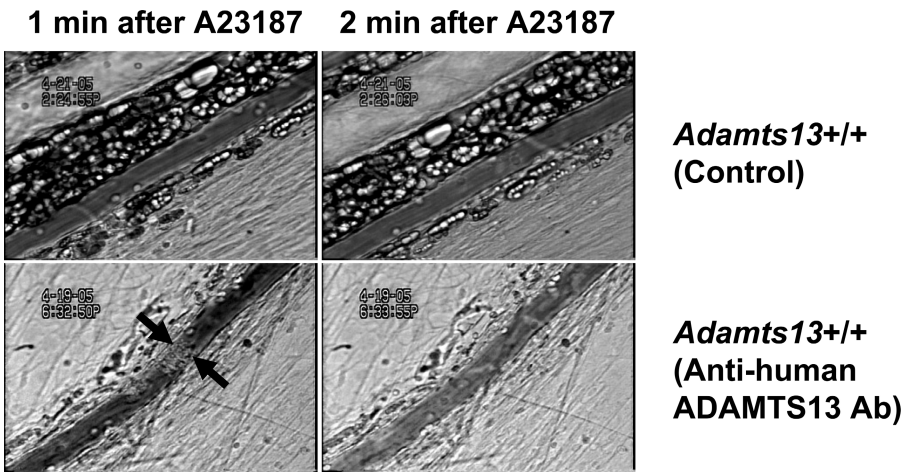

Figure 3. Thrombus formation in microvenules of *Adamts13*$^{+/+}$ mice infused with an anti–ADAMTS13 antibody. Mesenteric venules of ~25–30-μm in diameter were observed. 1 min after topical superfusion with A23187, thrombus formation was observed in four out of six *Adamts13*$^{+/+}$ mice infused with the anti-ADAMTS13 Ab. The microthrombi formation and embolization were similar to that seen in *Adamts13*$^{-/-}$ mice (Fig. 1). Arrows indicate a microthrombus. Microthrombi did not form in *Adamts13*$^{+/+}$ control ($n = 5$).

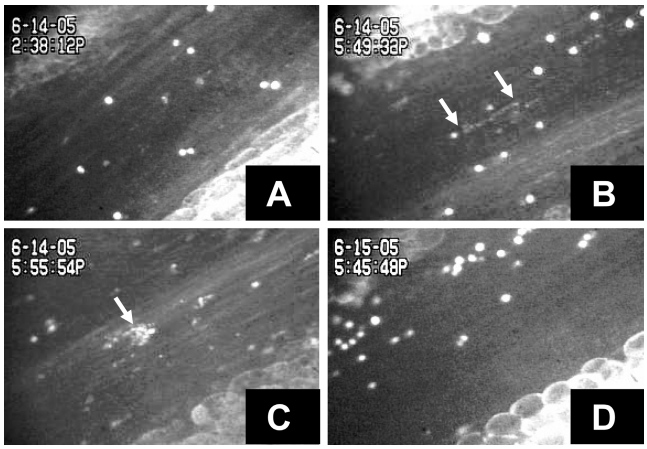

Figure 4. Recombinant ADAMTS13 inhibits platelet strings in *Adamts13*$^{-/-}$ mice. Rhodamine 6G was used to label endogenous platelets and leukocytes. Histamine was administered i.p. 15 min before surgery and three mesenteric venules of ~200–300 μm in diameter were visualized per mouse. (A) No platelet strings are seen in *Adamts13*$^{+/+}$ mice ($n = 5$). (B) Platelet strings (indicated by arrows) are seen in the *Adamts13*$^{-/-}$ mice. Platelet strings anchor up to 1 min on the endothelium ($n = 5$). (C) The platelet strings could form platelet aggregates in *Adamts13*$^{-/-}$ mice as indicated by arrow. (D) Infusion of r-hu ADAMTS13 protein inhibits the platelet strings in *Adamts13*$^{-/-}$ mice ($n = 4$).

were either not seen or were very short lived (<2 s) in the *Adamts13*$^{+/+}$ mice.

ADAMTS13 inhibitor induces thrombi formation in microvenules of *Adamts13*$^{+/+}$ mice

In the *Adamts13*$^{+/+}$ mice infused with anti–human ADAMTS13 antibody 2 h before surgical preparation, microthrombi formed on the vessel wall 45 s to 1 min after topical superfusion of A23187 in four out of six mice (Fig. 3). The microthrombi appearance was similar to those seen in the *Adamts13*$^{-/-}$ mice (Fig. 1). In control *Adamts13*$^{+/+}$ mice, short-lived platelet strings could be seen attached to the endothelium, but they did not result in thrombus formation ($n = 5$).

Histamine promotes platelet string formation in the venules of *Adamts13*$^{-/-}$ mice, a process inhibited by recombinant ADAMTS13

Histamine produced during inflammation is a secretagogue of Weibel-Palade bodies and stimulates the endothelium (29). We investigated whether activation of venules by injecting histamine i.p. into *Adamts13*$^{-/-}$ mice could result in platelet strings. Endogenous platelets were labeled by infusing Rhodamine 6G i.v. before surgery. Histamine was injected i.p. 15 min before the surgical preparation into *Adamts13*$^{-/-}$ ($n = 5$) and *Adamts13*$^{+/+}$ ($n = 5$) mice and venules at a shear rate of ~100 s^{-1} were visualized. In the *Adamts13*$^{+/+}$ mice, strings of platelets were not seen or were short lived (<5 s; Fig. 4 A), whereas, in the *Adamts13*$^{-/-}$ platelet strings, varying from 20 to 100 μm could be seen (Fig. 4 B) anchored to the endothelium for ~1 min. In some mice, the platelet strings persisted for up to 5 min. Some strings appeared to coalesce, forming aggregates (Fig. 4 C) that were later released into the blood stream. Infusion of r-hu ADAMTS13 protein in the *Adamts13*$^{-/-}$ mice ($n = 4$; 3 venules per mouse) inhibited platelet string formation in all venules examined (Fig. 4 D), thus demonstrating the activity of ADAMTS13 at low shear.

Platelet binding to subendothelium is increased in *Adamts13*$^{-/-}$ mice

Ferric chloride ($FeCl_3$) injury leads to deendothelization and exposes subendothelium (30). Platelet subendothelial interactions after injury at arterial shear are initiated by GPIb–VWF interaction and propagated by other receptors (30). In both *Adamts13*$^{+/+}$ and *Adamts13*$^{-/-}$ mice, platelet–vessel wall interaction started rapidly after $FeCl_3$ application to the arteriole. The number of animals in which >100 fluorescent platelets were deposited 2–3 min after injury was higher in *Adamts13*$^{-/-}$ mice. In the *Adamts13*$^{-/-}$, 7 out of 12 mice showed >100 platelets deposited on the vessel wall compared with 3 out of 10 in the *Adamts13*$^{+/+}$ mice ($P < 0.05$, Fig. 5 A).

Thrombus formation is accelerated in injured arterioles of *Adamts13*$^{-/-}$ mice

After finding that ADAMTS13 negatively modulates resting platelet adhesion to both stimulated endothelium and subendothelium, we asked whether the enzyme affects arteriolar thrombus formation. This process requires platelet activation and employs several ligands aside from VWF (30). The shear rate and diameter of arterioles studied were similar for *Adamts13*$^{-/-}$ and *Adamts13*$^{+/+}$ mice (Table I). In the *Adamts13*$^{-/-}$ mice, thrombi grew faster as thrombi >30 μm were seen at 6.64 ± 0.93 min compared with 10.78 ± 0.80 min in the *Adamts13*$^{+/+}$ mice ($P < 0.005$, Fig. 5 B). This suggests that cleavage of VWF multimers by ADAMTS13 delays thrombus formation. The thrombi grew to occlusive size in 10.56 ± 0.72 min in *Adamts13*$^{-/-}$ mice, whereas in *Adamts13*$^{+/+}$ mice all the vessels were still open at this time (Fig. 5, C and D). In the *Adamts13*$^{+/+}$, the mean vessel occlusion time was 16.69 ± 1.25 min after injury ($P < 0.0005$). All the vessels occluded at the site of injury. Of note, in arterioles of *Adamts13*$^{-/-}$ mice, the mean time for formation of thrombi (>30 μm) as well as the mean occlusion time were less than that of any individual *Adamts13*$^{+/+}$ mouse (Fig. 5, B and C).

ADAMTS13 deficiency enhances thrombus growth in an αIIbβ3 integrin-dependent manner

To study the importance of integrin αIIbβ3 for thrombus formation in the absence of *ADAMTS13*, we performed in vitro flow chamber studies with whole blood in the presence or absence of a blocking antibody (JON/A) against αIIbβ3 (31) (Fig. 6). To quantify the size of the thrombi, the surface area covered by fluorescently labeled platelets was determined. As expected, *Adamts13*$^{-/-}$ blood formed significantly

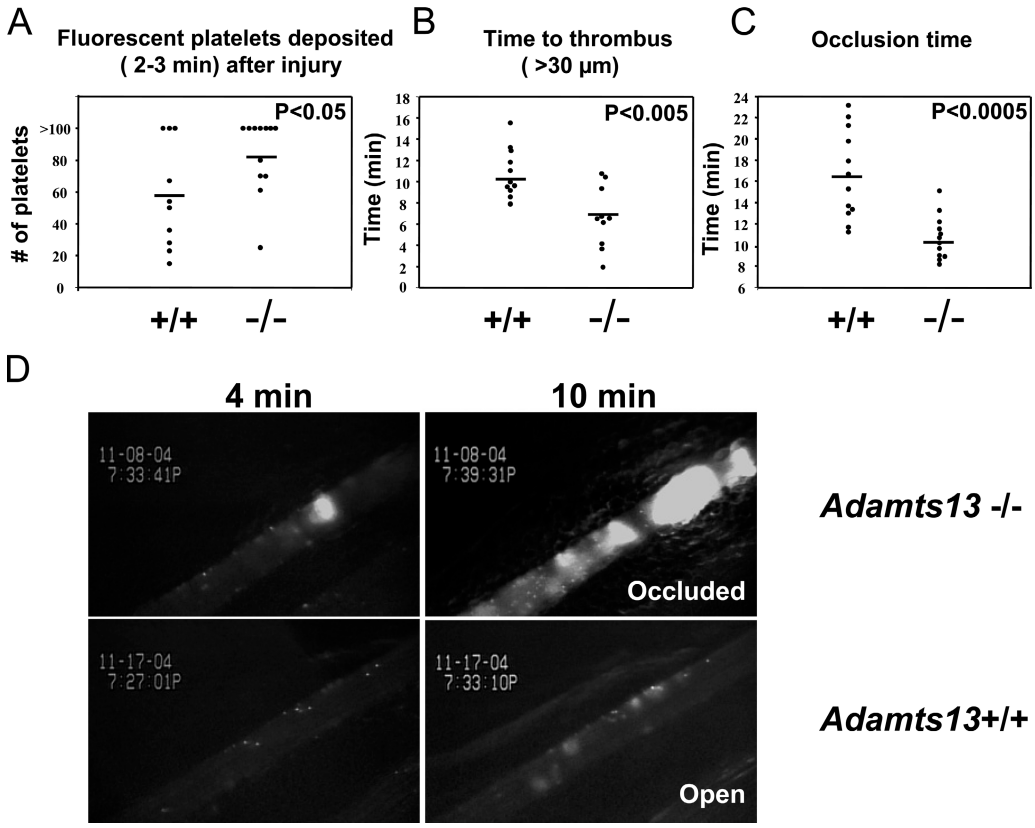

Figure 5. Quantitative analysis of platelet adhesion and thrombi formation in $FeCl_3$-injured arterioles of *Adamts13*$^{+/+}$ and *Adamts13*$^{-/-}$ mice. (A) The number of fluorescent platelets deposited per minute was determined in the interval 2–3 min after injury. Absence of ADAMTS13 in the plasma significantly increases early platelet interaction with the subendothelium ($P < 0.05$). (B) Thrombi (>30 μm) appeared sooner in *Adamts13*$^{-/-}$ mice compared with *Adamts13*$^{+/+}$ ($P < 0.005$). (C) The occlusion time (blood flow completely stopped for 10 s) was determined. Both *Adamts13*$^{+/+}$ and *Adamts13*$^{-/-}$ mice occluded at the site of injury; however, in *Adamts13*$^{-/-}$ mice, occlusion time was shorter as compared with *Adamts13*$^{+/+}$ mice ($P < 0.0005$). (D) Fluorescently labeled platelets representing ~2.5% of total platelets were observed in mesenteric arterioles of live mice after $FeCl_3$ injury. Single adherent platelets are seen in the arteriole at 4 min after injury in the *Adamts13*$^{+/+}$ mouse, whereas a thrombus (~30 μm) can already be seen in the *Adamts13*$^{-/-}$ mouse at the same time point. The vessel was occluded at 10 min at the site of injury in the *Adamts13*$^{-/-}$ mouse, whereas the *Adamts13*$^{+/+}$ mouse arteriole remained opened at that time. Representative figures are shown. Blood flow was from left to right.

larger thrombi than *Adamts13*$^{+/+}$ when perfused over collagen for 2 min at a shear rate of 1,500 s^{-1} (44.66 ± 3.63% vs. 20.22 ± 3.88%; $P < 0.0005$), demonstrating again the key role of *ADAMTS13* in limiting thrombus growth. In the presence of the blocking antibody to αIIbβ3, only single platelets adhered to the collagen surface and thrombus formation was completely inhibited in both the *Adamts13*$^{+/+}$ and *Adamts13*$^{-/-}$ blood (3.01 ± 0.97% vs. 2.82 ± 0.39%; $P > 0.05$).

In addition, we tested whether infusion of ADAMTS13 inhibitory antibody into β3 integrin-deficient mice (32) would induce thrombus formation after $FeCl_3$ injury. We could not detect any thrombi in injured arterioles of β3$^{-/-}$ mice (three animals were evaluated) despite the presence of the anti-ADAMTS13 antibody (unpublished data). Collectively, these results indicate that, at the arterial shear rates, UL-VWF enhances thrombus growth in an αIIbβ3-dependent manner.

Infusion of r-hu ADAMTS13 into *Adamts13*$^{-/-}$ or wild-type (C57BL/6J) mice inhibits thrombus growth by destabilizing the platelet aggregate

In vitro, r-hu ADAMTS13 cleaves human VWF (18) and mouse plasma VWF into proteolytic fragments with the same efficiency (unpublished data). It has been demonstrated that r-hu ADAMTS13 corrects the VWF cleavage defect in hereditary TTP plasma (33). Because we observed accelerated growth of thrombi in *Adamts13*$^{-/-}$ mice, we hypothesized that ADAMTS13 negatively modulates thrombus growth and, therefore, infusion of r–hu ADAMTS13 could delay thrombus formation. We infused r-hu ADAMTS13 into mice and determined that the concentration of the circulating human protein was ~8.8 U/ml at 17 min after infusion and 1.1 U/ml at 53 min after infusion. These times correspond approximately to the onset of $FeCl_3$ injury and the termination of the experiment. We examined first whether the prothrombotic phenotype of *Adamts13*$^{-/-}$ mice could be reversed. In 5 out

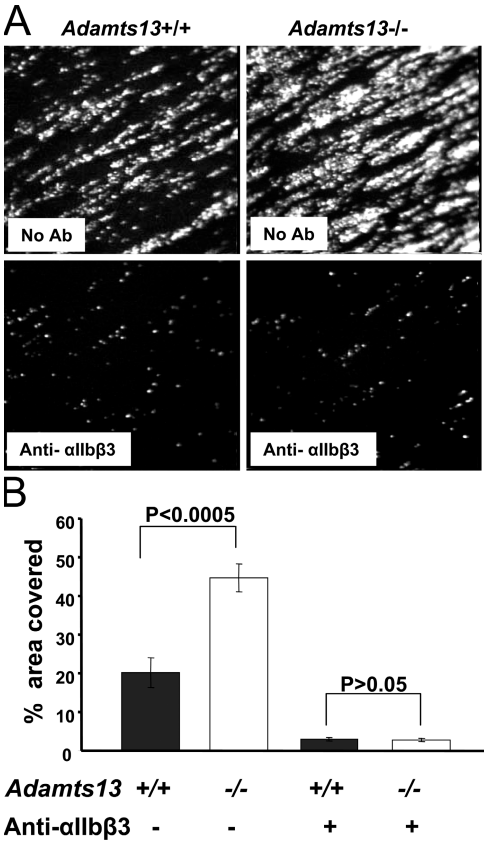

Figure 6. Inhibition of integrin αIIbβ3 blocks thrombus formation of ADAMTS13$^{-/-}$ platelets on collagen under arterial shear rate conditions. *Adamts13*$^{+/+}$ or *Adamts13*$^{-/-}$ whole blood was perfused for 2 min over a collagen surface at a shear rate of 1, 500 s^{-1}. (A) Representative images are shown. (top) Untreated whole blood; (bottom) whole blood pretreated with blocking antibody against αIIbβ3 (JON/A). (B) Quantification of the surface area covered by platelets after 2 min of perfusion. Four frames from different areas of the flow chamber were analyzed for each blood sample. Data represent the mean percentage of surface area covered by fluorescent platelets ± SEM (n = 3–4).

of 13 *Adamts13*$^{-/-}$ mice infused with r-hu ADAMTS13, injured arterioles did not occlude for up to 40 min when the experiment was terminated (Fig. 7 A). The effect of the infused r-hu ADAMTS13 was more than that of endogenous ADAMTS13 in *Adamts13*$^{+/+}$ mice; as in this injury model, all *Adamts13*$^{+/+}$ vessels occluded at <24 min (Fig. 5 C). The mean occlusion time was significantly prolonged in comparison with the control mice infused with buffer ($P < 0.0005$). In all the mice whose arterioles did not occlude, thrombi formed but were unstable and dissolved (Fig. 7 C). This phenomenon of thrombi formation and destabilization was present during the entire period of observation.

To examine whether r-hu ADAMTS13 could delay occlusion in injured arterioles of mice with normal levels of the endogenous ADAMTS13 protein, we infused the recombinant protein in C57BL/6J wild-type mice before injury. The infused protein caused significant delay in occlusion time with half of the arterioles not occluding by 40 min, whereas all arterioles of wild-type mice infused with vehicle occluded by 15 min (Fig. 7 B, $P < 0.008$). Thus, ADAMTS13 appears to have a significant antithrombotic potential even in wild-type animals.

DISCUSSION

The studies presented here have defined a key role for ADAMTS13 in preventing thrombi formation in activated microvenules and excessive thrombus formation in the injured arterioles of mice. Our in vivo findings of microvascular thrombosis caused by stimulated release of VWF are consistent with the observation that patients suffering from TTP have thrombi rich in platelet aggregates and VWF (27). It was suggested that, in the development of TTP, microvascular endothelial activation could be the primary event initiating platelet aggregation in the arterioles and capillaries (2). Various agents, including viruses, bacterial shiga toxins, drugs such as ticlopidine and clopidogrel, antibodies, and immune complexes, can trigger vascular activation (34), perhaps inducing Weibel-Palade body release. We did not see thrombi in the arterioles (which have higher shear stress) treated identically with A23187. This is because either Weibel-Palade bodies were not released in these vessels or, more likely, VWF is washed too quickly from the endothelial surface to promote platelet adhesion. Venous thrombosis is not generally recognized as a pathologic characteristic of TTP in human patients and was also not a prominent feature of spontaneous or shigatoxin-induced TTP in the *Adamts13*$^{-/-}$ mouse (26). These observations suggest that formation of platelet-rich microthrombi in the venous circulation in the setting of acute TTP is either subclinical or transient, or counterbalanced by other regulatory processes that are not as effective in the arteriolar vasculature.

Autoantibodies neutralizing human ADAMTS13 are the major cause of acquired TTP. Various epitopes of the ADAMTS13 protein are recognized by the autoantibodies (35, 36). Infusion of anti-ADAMTS13 antibody in the *Adamts13*$^{+/+}$ mice resulted in prolonged adhesion of platelets to secreted VWF and platelet string formation on the stimulated endothelium (Fig. 2) that was similar to that seen in the *Adamts13*$^{-/-}$ mice (26). It was shown that P-selectin may anchor the newly released UL-VWF multimers in vitro (37); however, this remains to be confirmed in vivo. Platelet strings and aggregates were frequently seen in the *Adamts13*$^{-/-}$ mice when challenged with Weibel-Palade body secretagogues (unpublished data) such as histamine (38), the inflammatory cytokine TNF-α (39), or activated platelets (40). This suggests that in patients lacking functional ADAMTS13, TTP could be precipitated by inflammation, by allergic responses, or by situations leading to platelet activation. Infusion of anti-ADAMTS13 antibody into *Adamts13*$^{+/+}$ mice with activated microvenules resulted in platelet aggregation and thrombi formation (Fig. 3). However, these thrombi embolized rapidly, similar to those in the *Adamts13*$^{-/-}$ mice. Thus, the mouse infused with anti-ADAMTS13 antibody represents a new animal model for acquired TTP.

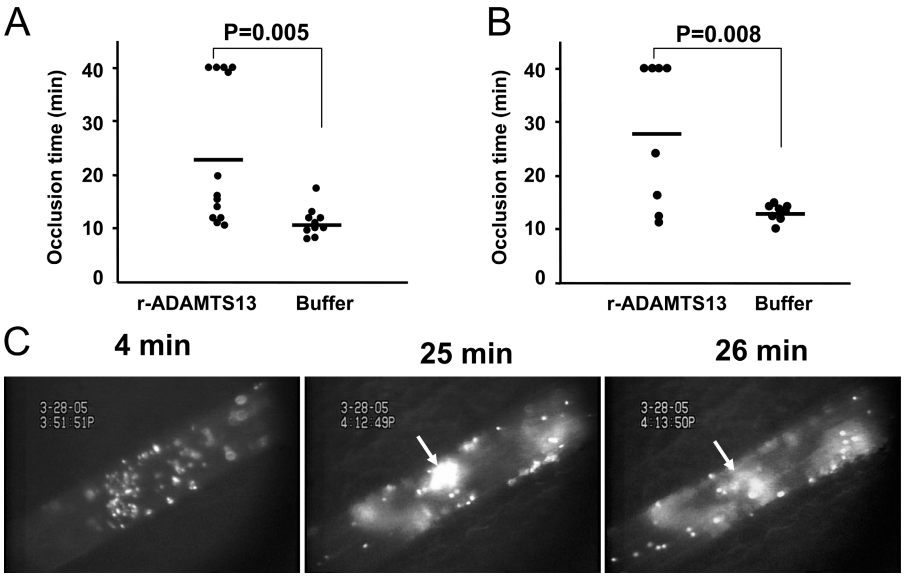

Figure 7. Infusion of r-hu ADAMTS13 inhibits thrombus growth. r-hu ADAMTS13 was infused i.v. into the *Adamts13*$^{-/-}$ mice 15 min before the $FeCl_3$ injury. The occlusion time (blood flow completely stopped for 10 s) was determined. (A) 5 out of 13 *Adamts13*$^{-/-}$ mice infused with r-hu ADAMTS13 did not occlude in the arteriole at up to 40 min of observation time (mean occlusion time = 23.80 ± 3.71 min), whereas all 10 *Adamts13*$^{-/-}$ mice infused with recombinant buffer occluded (mean occlusion time = 11.17 ± 0.87 min, P = 0.005). (B) Occlusion time in injured arterioles of WT (C57BL/6J) mice infused either with r-hu ADAMTS13 (mean occlusion time = 27.99 ± 4.72 min) or buffer (mean occlusion time = 13.12 ± 0.55 min) alone. (C) Representative fluorescent images of an injured arteriole of an *Adamts13*$^{-/-}$ mouse treated with r-hu ADAMTS13 are shown. Arrows indicate a dissolving thrombus. See Video 2 (available at http://www.jem.org/cgi/content/full/jem.20051732/DC1) for the effect of r-hu ADAMTS13 on thrombus growth.

Our observations that endothelial activation of microvenules results in thrombi in the *Adamts13*$^{-/-}$ mice led to the hypothesis that ADAMTS13 deficiency might accelerate thrombus formation in injured arterioles. Indeed, the absence of ADAMTS13 promoted all aspects of thrombus growth. Unexpectedly, even more platelets were deposited on the denuded vessel wall after 2–3 min of injury in the *Adamts13*$^{-/-}$ mice as compared with *Adamts13*$^{+/+}$ (Fig. 5 A). Because early platelet deposition in arterioles is VWF dependent (30), it means that either plasma ADAMTS13 reduces VWF incorporation into the basement membrane when it is exposed to blood or that it digests VWF already present in the extracellular matrix. The rapid thrombus growth and occlusion in *Adamts13*$^{-/-}$ mice indicates that ADAMTS13 might cleave VWF multimers incorporated in the thrombus. It has been suggested that cleavage of VWF domain A2 by ADAMTS13 is facilitated by the binding of VWF to GPIbα (41). Thus, the VWF–GPIb interaction within the thrombus may negatively regulate thrombus growth. Thrombus formation under venous and arterial flow conditions also depends on major integrin αIIbβ3 (42, 43). Our studies at arteriolar shear rates show that ADAMTS13 modulates the growing thrombus only when platelets in the thrombus express an active β3 integrin. Under our in vitro and in vivo experimental conditions, ADAMTS13 deficiency did not promote thrombus growth if the major platelet integrin was absent or inhibited (Fig. 6).

To inhibit the fast thrombus growth seen in the *Adamts13*$^{-/-}$ mice, we infused r-hu ADAMTS13 into the *Adamts13*$^{-/-}$ and wild-type mice before injury. The antithrombotic effect of the r-hu ADAMTS13, although highly statistically significant, varied among the animals (Fig. 7). Some mice did not respond to r-hu ADAMTS13 treatment. It is possible that in these mice r-hu ADAMTS13 was proteolytically inactivated by thrombin and plasmin (44) produced at the sites of vascular injury. IL-6 (39) and high amounts of VWF released after inflammation (45) or injury could also reduce ADAMTS13 activity. Infusion of the r-hu ADAMTS13 protein into the histamine-challenged *Adamts13*$^{-/-}$ mice inhibited platelet string and aggregate formation in the activated venules. In vivo, similar to in vitro (46), ADAMTS13 appears to interact with endothelial UL-VWF. Collectively, our findings suggest that ADAMTS13 could have both antithrombotic as well as thrombo-destabilizing activity. In the thrombus, ADAMTS13 could be cleaving the UL-VWF multimers released from platelets into less adhesive smaller fragments and/or directly cleaving the VWF molecules bridging the platelets. However, we also cannot exclude the possibility that there may be another substrate for ADAMTS13 that is important in thrombus formation.

In summary, our results suggest that in vivo ADAMTS13 is active at both low venous and high arterial shear stress conditions. It cleaves platelet strings and regulates platelet interaction with the "activated" vessel wall in the venules, prevents thrombi in activated microvenules, and modulates the thrombotic response in injured arterioles. The antithrombotic effect of ADAMTS13 suggests that in addition to TTP, recombinant

ADAMTS13 could also be used to treat patients suffering from thrombotic disorders as a result of other hereditary defects, inflammatory disease, or septic conditions.

MATERIALS AND METHODS

Animals. Mice used in this study were siblings obtained from crosses of *Adamts13*$^{+/-}$ mice on C57BL/6J/129Sv background (26). The mice of pure C57BL/6J background were purchased from The Jackson Laboratory and β3 integrin$^{-/-}$ mice (32) on BALB/c background were a gift from R. Hynes (Massachusetts Institute of Technology, Cambridge, MA). The mice used for intravital microscopy were young mice (~4 wk old), both male and female, weighing 14–18 g. Infused platelets were isolated from 4–6-mo-old mice of the same genotype. Animals were bred and housed at the CBR Institute for Biomedical Research and all experimental procedures were approved by its Animal Care and Use Committee.

Blood sampling and platelet preparation. Blood was harvested from the retro-orbital venous plexus by puncture and collected in 1.5-ml polypropylene tubes containing 300 μl of heparin (30 U/ml). Platelet-rich plasma was obtained by centrifugation at 1,200 revolutions/min for 5 min. The plasma and buffy coat containing some RBCs were gently transferred to fresh polypropylene tubes and recentrifuged at 1,200 revolutions/min for 5 min. The platelet-rich plasma was transferred to fresh tubes containing 2 μl of PGI_2 (2 μg/ml) and incubated at 37°C for 5 min. After centrifugation at 2,800 revolutions/min, pellets were resuspended in 1 ml of modified Tyrode-Hepes buffer (137 mM NaCl, 0.3 mM Na_2HPO_4, 2 mM KCl, 12 mM $NaHCO_3$, 5 mM Hepes, 5 mM glucose, 0.35% BSA) containing 2 μl of PGI_2 and incubated at 37°C for 5 min. The suspended pellet was centrifuged at 2,800 revolutions/min for 5 min. To remove PGI_2, the washing step was repeated twice and platelets were fluorescently labeled with calcein AM 2.5 μg/ml (Invitrogen) for 10 min at room temperature.

Polyclonal anti-ADAMTS13 production and purification. Polyclonal rabbit anti–human ADAMTS13 IgG was produced by Baxter Bioscience. The antibody was obtained by immunization of New Zealand white rabbits with purified r-hu ADAMTS13, COOH-terminally tagged with six His residues. Two rabbits were immunized by injection of 20 μg of r-hu ADAMTS13 (6-His) in 200 μl of complete Freund's adjuvant. The animals were boostered after 2, 4, and 6 wk by injecting 20 μg of r-hu ADAMTS-13 (6-His) in 200 μl of incomplete Freund's adjuvant. After 8 wk, the rabbits were killed and bled. IgG antibodies were purified by protein G affinity chromatography (HiTrap protein G HP column; GE Healthcare) and formulated in PBS.

Thrombosis in microvenules. Intravital microscopy was as performed as described previously (47). In brief, mice were anesthetized with 2.5% tribromoethanol (0.15 ml/10 g) and an incision was made through the abdominal wall to expose the mesentery and a mesenteric venule of 25–30-μm diameter was studied. Exposed mesentery was kept moist by periodic superfusion using PBS (without Ca^{2+} or Mg^{2+}) warmed to 37°C. The shear rate was calculated using an optical Doppler velocity meter (48). Venules were visualized using an Axiovert 135 inverted microscope (objectives: 10× and 32×; Carl Zeiss MicroImaging, Inc.) connected to an SVHS video recorder (AG-6730; Panasonic). One venule was chosen per mouse and filmed for 3 min for the baseline before the A23187 superfusion (30 μl of a 10 μmol/L solution) and monitored for 10 min.

Platelet adhesion in large venules. Intravital microscopy was performed as described previously (28), except mesenteric venules of 200–300-μm diameters were studied. Fluorescent platelets (1.25×10^9 platelets/kg) were infused through the tail vein. One venule per animal was filmed for 3 min for the baseline before the A23187 superfusion (30 μl of a 10 μmol/L solution) and filming continued until after the platelet sticking and rolling returned to baseline. Purified rabbit polyclonal anti–human ADAMTS13 antibody (5 mg/kg mouse) was dissolved in PBS. Control rabbit IgG (Sigma-Aldrich) was dissolved in PBS. 200 μl of 1 mM histamine (Sigma-Aldrich) was injected i.p. to stimulate the endothelium. 100 μl (0.2 mg/ml) of Rhodamine 6G (Sigma-Aldrich) was injected i.v. to label the endogenous platelets and leukocytes before surgery and imaging.

Thrombus in arterioles. A previously described model was used with slight modifications (30). In brief, mice were anesthetized with 2.5% tribromoethanol (0.15 ml/10 g) and fluorescent platelets (1.25×10^9 platelets/kg) were infused through the retro-orbital plexus of the eye. An incision was made through the abdominal wall to expose the mesentery, and arterioles of ~100 μm diameter were studied. The shear rate was calculated as described previously (48). Arterioles were visualized using the aforementioned microscope, equipped with a 100-W HBO fluorescent lamp source (Optic Quip). Whatman paper saturated with $FeCl_3$ (10%) solution was applied topically for 5 min, which induced denudation of the endothelium, and the vessel was monitored for 40 min after injury or until occlusion. One arteriole was chosen per mouse.

Quantitative analysis of arteriolar thrombus. Analysis of the recorded tape was performed blinded to the genotype. We evaluated (1) single platelet–vessel wall interaction determined as the number of fluorescent platelets that deposited on the 250 μm vessel wall segment during 1 min (2–3 min after injury). Quantitative analysis was performed using the following factors: platelet counts >100 were counted as 100 for statistics, (2) the time required for formation of a thrombus >30 μm, (3) thrombus stability by determining the number of thrombi of diameter >30 μm embolizing before vessel occlusion, (4) occlusion time of the vessel, that is, time required for blood to stop flowing for 10 s, and (5) site of vessel occlusion, that is, at the site of injury or downstream.

r-hu ADAMTS13 infusion. r-hu ADAMTS13 protein was dissolved in 150 mmol NaCl/20 mmol histidin/2% sucrose/0.05% Crillet 4HP, Tween 80, pH 7.4 (Baxter Bioscience). r-hu ADAMTS13 (3,460 U/kg mouse) was injected i.v. Levels of human ADAMTS13 antigen were determined by a slight modification of the ELISA method described by Rieger et al. (49) and r-hu ADAMTS13 activity was determined according to Gerristen et al. (50). 1 U corresponds to the level of ADAMTS13 activity in pooled normal human plasma.

Flow chamber studies. Flow chamber studies were performed as described previously (51). In brief, platelets were isolated from heparinized whole blood, washed in modified Tyrode-Hepes buffer, and labeled with 2.5 μg/ml calcein. Platelet-poor whole blood was reconstituted with labeled platelets before perfusion in a parallel-plate flow chamber system coated with 100 μg/ml collagen Horm (NYCOMED) for 1 h at room temperature. Where indicated, samples were pretreated with 30 μg/ml JON/A (emfret Analytics) (31) for 10 min before perfusion. Platelet adhesion was visualized with an Axiovert 135 inverted microscope (Carl Zeiss MicroImaging, Inc.). The percentage of surface area covered by fluorescent platelets was analyzed using National Institutes of Health Image 1.61 software by an individual blinded to genotypes.

Statistical analysis. Results are reported as the mean ± SEM. The statistical significance of the difference between means was assessed by the Student's *t* test.

Online supplemental material. Video 1 shows stimulated release of Weibel-Palade bodies in a microvenule of an ADAMTS13$^{-/-}$ mouse leads to rapid formation of thrombi that embolize downstream. Video 2 depicts arteriolar injury in an ADAMTS13$^{-/-}$ mouse that results in rapid vessel occlusion and infusion of r-hu ADAMTS13 inhibits thrombus growth. Online supplemental material is available at http://www.jem.org/cgi/content/full/jem.20051732/DC1.

We thank L. Cowan for help in preparing the manuscript.

This work was supported by the National Institutes of Health, National Heart, Lung, and Blood Institute grant nos. R37 HL41002 (to D.D. Wagner) and R01

HL39693 and P01 HL057346 (to D. Ginsburg). D. Ginsburg is a Howard Hughes Medical Institute Investigator.

M. Dockal, B. Plaimauer, and F. Scheiflinger are employees of Baxter Bioscience. The authors have no other conflicting interests.

Submitted: 25 August 2005
Accepted: 10 February 2006

REFERENCES

1. Sadler, J.E., J.L. Moake, T. Miyata, and J.N. George. 2004. Recent advances in thrombotic thrombocytopenic purpura. *Hematology (Am. Soc. Hematol. Educ. Program)*. 2004:407–423.
2. Moake, J.L. 2002. Thrombotic microangiopathies. *N. Engl. J. Med.* 347:589–600.
3. Moake, J.L., C.K. Rudy, J.H. Troll, M.J. Weinstein, N.M. Colannino, J. Azocar, R.H. Seder, S.L. Hong, and D. Deykin. 1982. Unusually large plasma factor VIII:von Willebrand factor multimers in chronic relapsing thrombotic thrombocytopenic purpura. *N. Engl. J. Med.* 307:1432–1435.
4. Furlan, M., R. Robles, M. Galbusera, G. Remuzzi, P.A. Kyrle, B. Brenner, M. Krause, I. Scharrer, V. Aumann, U. Mittler, et al. 1998. von Willebrand factor-cleaving protease in thrombotic thrombocytopenic purpura and the hemolytic-uremic syndrome. *N. Engl. J. Med.* 339:1578–1584.
5. Furlan, M., R. Robles, M. Solenthaler, M. Wassmer, P. Sandoz, and B. Lammle. 1997. Deficient activity of von Willebrand factor-cleaving protease in chronic relapsing thrombotic thrombocytopenic purpura. *Blood.* 89:3097–3103.
6. Tsai, H.M., and E.C. Lian. 1998. Antibodies to von Willebrand factor-cleaving protease in acute thrombotic thrombocytopenic purpura. *N. Engl. J. Med.* 339:1585–1594.
7. Furlan, M., R. Robles, and B. Lamie. 1996. Partial purification and characterization of a protease from human plasma cleaving von Willebrand factor to fragments produced by in vivo proteolysis. *Blood.* 87:4223–4234.
8. Tsai, H.M. 1996. Physiologic cleavage of von Willebrand factor by a plasma protease is dependent on its conformation and requires calcium ion. *Blood.* 87:4235–4244.
9. Furlan, M., R. Robles, M. Solenthaler, and B. Lammle. 1998. Acquired deficiency of von Willebrand factor-cleaving protease in a patient with thrombotic thrombocytopenic purpura. *Blood.* 91:2839–2846.
10. Levy, G.G., W.C. Nichols, E.C. Lian, T. Foroud, J.N. McClintick, B.M. McGee, A.Y. Yang, D.R. Siemieniak, K.R. Stark, R. Gruppo, et al. 2001. Mutations in a member of the ADAMTS gene family cause thrombotic thrombocytopenic purpura. *Nature.* 413:488–494.
11. Soejima, K., N. Mimura, M. Hirashima, H. Maeda, T. Hamamoto, T. Nakagaki, and C. Nozaki. 2001. A novel human metalloprotease synthesized in the liver and secreted into the blood: possibly, the von Willebrand factor-cleaving protease? *J. Biochem. (Tokyo).* 130:475–480.
12. Zheng, X., D. Chung, T.K. Takayama, E.M. Majerus, J.E. Sadler, and K. Fujikawa. 2001. Structure of von Willebrand factor-cleaving protease (ADAMTS13), a metalloprotease involved in thrombotic thrombocytopenic purpura. *J. Biol. Chem.* 276:41059–41063.
13. Uemura, M., K. Tatsumi, M. Matsumoto, M. Fujimoto, T. Matsuyama, M. Ishikawa, T.A. Iwamoto, T. Mori, A. Wanaka, H. Fukui, and Y. Fujimura. 2005. Localization of ADAMTS13 to the stellate cells of human liver. *Blood.* 106:922–924.
14. Zhou, W., M. Inada, T.P. Lee, D. Benten, S. Lyubsky, E.E. Bouhassira, S. Gupta, and H.M. Tsai. 2005. ADAMTS13 is expressed in hepatic stellate cells. *Lab. Invest.* 85:780–788.
15. Scheiflinger, F., P. Knobl, B. Trattner, B. Plaimauer, G. Mohr, M. Dockal, F. Dorner, and M. Rieger. 2003. Nonneutralizing IgM and IgG antibodies to von Willebrand factor-cleaving protease (ADAMTS-13) in a patient with thrombotic thrombocytopenic purpura. *Blood.* 102:3241–3243.
16. Sporn, L.A., V.J. Marder, and D.D. Wagner. 1986. Inducible secretion of large, biologically potent von Willebrand factor multimers. *Cell.* 46:185–190.
17. Dent, J.A., M. Galbusera, and Z.M. Ruggeri. 1991. Heterogeneity of plasma von Willebrand factor multimers resulting from proteolysis of the constituent subunit. *J. Clin. Invest.* 88:774–782.
18. Plaimauer, B., K. Zimmermann, D. Volkel, G. Antoine, R. Kerschbaumer, P. Jenab, M. Furlan, H. Gerritsen, B. Lammle, H.P. Schwarz, and F. Scheiflinger. 2002. Cloning, expression, and functional characterization of the von Willebrand factor-cleaving protease (ADAMTS13). *Blood.* 100:3626–3632.
19. Zimmerman, T.S., J.A. Dent, Z.M. Ruggeri, and L.H. Nannini. 1986. Subunit composition of plasma von Willebrand factor. Cleavage is present in normal individuals, increased in IIA and IIB von Willebrand disease, but minimal in variants with aberrant structure of individual oligomers (types IIC, IID, and IIE). *J. Clin. Invest.* 77:947–951.
20. Dent, J.A., S.D. Berkowitz, J. Ware, C.K. Kasper, and Z.M. Ruggeri. 1990. Identification of a cleavage site directing the immunochemical detection of molecular abnormalities in type IIA von Willebrand factor. *Proc. Natl. Acad. Sci. USA.* 87:6306–6310.
21. Slayter, H., J. Loscalzo, P. Bockenstedt, and R.I. Handin. 1985. Native conformation of human von Willebrand protein. Analysis by electron microscopy and quasi-elastic light scattering. *J. Biol. Chem.* 260: 8559–8563.
22. Siedlecki, C.A., B.J. Lestini, K.K. Kottke-Marchant, S.J. Eppell, D.L. Wilson, and R.E. Marchant. 1996. Shear-dependent changes in the three-dimensional structure of human von Willebrand factor. *Blood.* 88:2939–2950.
23. Sporn, L.A., V.J. Marder, and D.D. Wagner. 1987. von Willebrand factor released from Weibel-Palade bodies binds more avidly to extracellular matrix than that secreted constitutively. *Blood.* 69:1531–1534.
24. Arya, M., B. Anvari, G.M. Romo, M.A. Cruz, J.F. Dong, L.V. McIntire, J.L. Moake, and J.A. Lopez. 2002. Ultralarge multimers of von Willebrand factor form spontaneous high-strength bonds with the platelet glycoprotein Ib-IX complex: studies using optical tweezers. *Blood.* 99:3971–3977.
25. Dong, J.F., J.L. Moake, L. Nolasco, A. Bernardo, W. Arceneaux, C.N. Shrimpton, A.J. Schade, L.V. McIntire, K. Fujikawa, and J.A. Lopez. 2002. ADAMTS-13 rapidly cleaves newly secreted ultralarge von Willebrand factor multimers on the endothelial surface under flowing conditions. *Blood.* 100:4033–4039.
26. Motto, D.G., A.K. Chauhan, G. Zhu, J. Homeister, C.B. Lamb, K.C. Desch, W. Zhang, H.M. Tsai, D.D. Wagner, and D. Ginsburg. 2005. Shigatoxin triggers thrombotic thrombocytopenic purpura in genetically susceptible ADAMTS13-deficient mice. *J. Clin. Invest.* 115:2752–2761.
27. Asada, Y., A. Sumiyoshi, T. Hayashi, J. Suzumiya, and K. Kaketani. 1985. Immunohistochemistry of vascular lesion in thrombotic thrombocytopenic purpura, with special reference to factor VIII related antigen. *Thromb. Res.* 38:469–479.
28. Andre, P., C.V. Denis, J. Ware, S. Saffaripour, R.O. Hynes, Z.M. Ruggeri, and D.D. Wagner. 2000. Platelets adhere to and translocate on von Willebrand factor presented by endothelium in stimulated veins. *Blood.* 96:3322–3328.
29. Wagner, D.D., and R. Bonfanti. 1991. von Willebrand factor and the endothelium. *Mayo Clin. Proc.* 66:621–627.
30. Ni, H., C.V. Denis, S. Subbarao, J.L. Degen, T.N. Sato, R.O. Hynes, and D.D. Wagner. 2000. Persistence of platelet thrombus formation in arterioles of mice lacking both von Willebrand factor and fibrinogen. *J. Clin. Invest.* 106:385–392.
31. Bergmeier, W., V. Schulte, G. Brockhoff, U. Bier, H. Zirngibl, and B. Nieswandt. 2002. Flow cytometric detection of activated mouse integrin αIIbβ3 with a novel monoclonal antibody. *Cytometry.* 48:80–86.
32. Hodivala-Dilke, K.M., K.P. McHugh, D.A. Tsakiris, H. Rayburn, D. Crowley, M. Ullman-Cullere, F.P. Ross, B.S. Coller, S. Teitelbaum, and R.O. Hynes. 1999. β3-integrin-deficient mice are a model for Glanzmann thrombasthenia showing placental defects and reduced survival. *J. Clin. Invest.* 103:229–238.
33. Antoine, G., K. Zimmermann, B. Plaimauer, M. Grillowitzer, J.D. Studt, B. Lammle, and F. Scheiflinger. 2003. ADAMTS13 gene defects in two brothers with constitutional thrombotic thrombocytopenic purpura and normalization of von Willebrand factor-cleaving protease activity by recombinant human ADAMTS13. *Br. J. Haematol.* 120:821–824.
34. Ruggenenti, P., M. Noris, and G. Remuzzi. 2001. Thrombotic microangiopathy, hemolytic uremic syndrome, and thrombotic thrombocytopenic purpura. *Kidney Int.* 60:831–846.

35. Soejima, K., M. Matsumoto, K. Kokame, H. Yagi, H. Ishizashi, H. Maeda, C. Nozaki, T. Miyata, Y. Fujimura, and T. Nakagaki. 2003. ADAMTS-13 cysteine-rich/spacer domains are functionally essential for von Willebrand factor cleavage. *Blood*. 102:3232–3237.
36. Klaus, C., B. Plaimauer, J.D. Studt, F. Dorner, B. Lammle, P.M. Mannucci, and F. Scheiflinger. 2004. Epitope mapping of ADAMTS13 autoantibodies in acquired thrombotic thrombocytopenic purpura. *Blood*. 103:4514–4519.
37. Padilla, A., J.L. Moake, A. Bernardo, C. Ball, Y. Wang, M. Arya, L. Nolasco, N. Turner, M.C. Berndt, B. Anvari, et al. 2004. P-selectin anchors newly released ultralarge von Willebrand factor multimers to the endothelial cell surface. *Blood*. 103:2150–2156.
38. Hamilton, K.K., and P.J. Sims. 1987. Changes in cytosolic Ca2+ associated with von Willebrand factor release in human endothelial cells exposed to histamine. Study of microcarrier cell monolayers using the fluorescent probe indo-1. *J. Clin. Invest.* 79:600–608.
39. Bernardo, A., C. Ball, L. Nolasco, J.F. Moake, and J.F. Dong. 2004. Effects of inflammatory cytokines on the release and cleavage of the endothelial cell-derived ultralarge von Willebrand factor multimers under flow. *Blood*. 104:100–106.
40. Dole, V.S., W. Bergmeier, H.A. Mitchell, S.C. Eichenberger, and D.D. Wagner. 2005. Activated platelets induce Weibel-Palade-body secretion and leukocyte rolling in vivo: role of P-selectin. *Blood*. 106:2334–2339.
41. Nishio, K., P.J. Anderson, X.L. Zheng, and J.E. Sadler. 2004. Binding of platelet glycoprotein Ibalpha to von Willebrand factor domain A1 stimulates the cleavage of the adjacent domain A2 by ADAMTS13. *Proc. Natl. Acad. Sci. USA*. 101:10578–10583.
42. Ruggeri, Z.M., J.A. Dent, and E. Saldivar. 1999. Contribution of distinct adhesive interactions to platelet aggregation in flowing blood. *Blood*. 94:172–178.
43. Savage, B., F. Almus-Jacobs, and Z.M. Ruggeri. 1998. Specific synergy of multiple substrate-receptor interactions in platelet thrombus formation under flow. *Cell*. 94:657–666.
44. Crawley, J.T., J.K. Lam, J.B. Rance, L.R. Mollica, J.S. O'Donnell, and D.A. Lane. 2005. Proteolytic inactivation of ADAMTS13 by thrombin and plasmin. *Blood*. 105:1085–1093.
45. Reiter, R.A., K. Varadi, P.L. Turecek, B. Jilma, and P. Knobl. 2005. Changes in ADAMTS13 (von-Willebrand-factor-cleaving protease) activity after induced release of von Willebrand factor during acute systemic inflammation. *Thromb. Haemost.* 93:554–558.
46. Dong, J.F., J.L. Moake, A. Bernardo, K. Fujikawa, C. Ball, L. Nolasco, J.A. Lopez, and M.A. Cruz. 2003. ADAMTS-13 metalloprotease interacts with the endothelial cell-derived ultra-large von Willebrand factor. *J. Biol. Chem.* 278:29633–29639.
47. Frenette, P.S., R.C. Johnson, R.O. Hynes, and D.D. Wagner. 1995. Platelets roll on stimulated endothelium in vivo: an interaction mediated by endothelial P-selectin. *Proc. Natl. Acad. Sci. USA*. 92:7450–7454.
48. Frenette, P.S., C. Moyna, D.W. Hartwell, J.B. Lowe, R.O. Hynes, and D.D. Wagner. 1998. Platelet-endothelial interactions in inflamed mesenteric venules. *Blood*. 91:1318–1324.
49. Rieger, M., S. Ferrari, J.A. Kremer Hovinga, C. Konetschny, A. Herzog, L. Koller, A. Weber, G. Remuzzi, M. Dockal, B. Plaimauer and F. Scheiflinger. 2006. Relation between ADAMTS13 activity and ADAMTS13 antigen levels in healthy donors and patients with thrombotic microangiopathies (TMA). *Thromb. Haemost.* 95:212–220.
50. Gerritsen, H.E., P.L. Turecek, H.P. Schwarz, B. Lammle, and M. Furlan. 1999. Assay of von Willebrand factor (vWF)-cleaving protease based on decreased collagen binding affinity of degraded vWF: a tool for the diagnosis of thrombotic thrombocytopenic purpura (TTP). *Thromb. Haemost.* 82:1386–1389.
51. Bergmeier, W., P.C. Burger, C.L. Piffath, K.M. Hoffmeister, J.H. Hartwig, B. Nieswandt, and D.D. Wagner. 2003. Metalloproteinase inhibitors improve the recovery and hemostatic function of in vitro-aged or -injured mouse platelets. *Blood*. 102:4229–4235.